AD

AD-E403 866

Technical Report ARMET-TR-17031

NONDESTRUCTIVE EXAMINATION OF INSIDE SURFACES OF SMALL HOLES IN A STEEL STRUCTURE USING A LASER SCAN TECHNIQUE

David Grasing
Adam Foltz
Ryan Hooke
Venkataraman Swaminathan
U.S. Army ARDEC
Picatinny Arsenal, NJ

Andrew Littlefield
U.S. Army ARDEC
Benét Laboratories
Watervliet, NY

April 2017

U.S. ARMY ARMAMENT RESEARCH, DEVELOPMENT AND ENGINEERING CENTER

Munitions Engineering Technology Center

Picatinny Arsenal, New Jersey

The views, opinions, and/or findings contained in this report are those of the author(s) and should not be construed as an official Department of the Army position, policy, or decision, unless so designated by other documentation.

The citation in this report of the names of commercial firms or commercially available products or services does not constitute official endorsement by or approval of the U.S. Government.

Destroy by any means possible to prevent disclosure of contents or reconstruction of the document. Do not return to the originator.

REPORT DOCUMENTATION PAGE

1. REPORT DATE (DD-MM-YYYY) April 2017	2. REPORT TYPE Final	3. DATES COVERED (From - To) January 2015 to March 2016

4. TITLE AND SUBTITLE NONDESTRUCTIVE EXAMINATION OF INSIDE SURFACES OF SMALL HOLES IN A STEEL STRUCTURE USING A LASER SCAN TECHNIQUE	5a. CONTRACT NUMBER
	5b. GRANT NUMBER
	5c. PROGRAM ELEMENT NUMBER

6. AUTHORS David Grasing, Adam Foltz, Ryan Hooke, and Venkataraman Swaminathan – U.S. Army ARDEC, Picatinny Arsenal, NJ Andrew Littlefield - U.S. Army ARDEC, Benét Laboratory, Watervliet, NY	5d. PROJECT NUMBER
	5e. TASK NUMBER
	5f. WORK UNIT NUMBER

7. PERFORMING ORGANIZATION NAME(S) AND ADDRESS(ES) U.S. Army ARDEC, METC U.S. Army ARDEC Fuze & Precision Benét Laboratory Armaments Directorate (RDAR-WSB-L) (RDAR-MEF) Watervliet, NY 12189-4000 Picatinny Arsenal, NJ 07806-5000	8. PERFORMING ORGANIZATION REPORT NUMBER

9. SPONSORING/MONITORING AGENCY NAME(S) AND ADDRESS(ES) U.S. Army ARDEC, ESIC Knowledge & Process Management (RDAR-EIK) Picatinny Arsenal, NJ 07806-5000	10. SPONSOR/MONITOR'S ACRONYM(S)
	11. SPONSOR/MONITOR'S REPORT NUMBER(S) Technical Report ARMET-TR-17031

12. DISTRIBUTION/AVAILABILITY STATEMENT
Approved for public release; distribution is unlimited.

13. SUPPLEMENTARY NOTES

14. ABSTRACT

This paper describes the application of a commercial off-the-shelf laser-based inspection system to nondestructively examine the internal surfaces of small holes ~6 mm in diameter and ~19 mm in length embedded in a tubular section made of high strength steel. Methods are developed to analyze the data after correcting for laser probe wander while scanning and applying signal processing techniques to extract the Abbott-Firestone curves of the surface features. The tubular sections were subjected to a safety and reliability test simulating storage conditions to withstand exposure to repeated cycles of extreme temperatures and humidity. The temperature extremes were +71° and -54°C, and a relative humidity of 95% was used at +71°C. Under these conditions, corrosion was induced in the steel and the formation of pits was suggested by the increase in the surface heights with the number of days of treatment. Further analysis of the pit distributions showed that (1) the pit density decreases monotonically with increasing pit depth, (2) the maximum pit depth beyond which the pit density is negligible increases with the number of treatment days, and (3) for a given pit depth below the maximum, the pit density increases with the number of treatment days. No surface defects such as cracks were observed in any of the sections even after the maximum number of 84 days of treatment.

15. SUBJECT TERMS

Laser scan   Abbott-Firestone curves   Internal surfaces   Small holes

16. SECURITY CLASSIFICATION OF:			17. LIMITATION OF ABSTRACT	18. NUMBER OF PAGES	19a. NAME OF RESPONSIBLE PERSON Venkataraman Swaminathan
a. REPORT U	b. ABSTRACT U	c. THIS PAGE U	SAR	21	19b. TELEPHONE NUMBER (Include area code) (973) 724-7455

CONTENTS

FIGURES

ACKNOWLEDGMENTS

INTRODUCTION

Nondestructive evaluation (NDE) of small spaces such as internal holes or pipes in engineering structures is generally a challenging task. The difficulty usually arises due to the small space to insert a probe and the consequent impediments to manipulate the probe in the tight space and acquire reliable data at high speed with precision and accuracy. Laser-based inspection systems have been reported for inspection of pipes of both large [~20 to 25 cm in diameter (refs. 1 and 2)] and small [<1 cm in diameter (ref. 3)]. In addition, a computer vision-based inspection system (ref. 4) and a three-dimensional vision inspection using structured light (ref. 5) have also been proposed for inspecting internal surfaces of holes that have a diameter of <1 cm. Notwithstanding these advances, the inspection of small spaces is further exacerbated if other surface imperfections such as stress corrosion pits are also present. In these circumstances, detection of surface flaws, such as cracks in small internal surfaces often initiated at corrosion pits (ref. 6), is almost impossible. Thus, unambiguous identification of surface flaws in the midst of corrosion pits and the derivation of accurate and reliable statistical parameters of their distribution are an important problem for routine NDE of small spaces. Herein, the application of a modified commercial-off-the-shelf (COTS) laser-based inspection system (ref. 3) to probe the internal surface textures of a <1-cm diameter hole inside a steel structure is described. Specifically, signal processing and data analysis techniques have been developed so as to derive reliable statistical parameters of the inside surface textures of the holes after correcting for laser probe wander and deviations in the geometry of the hole.

EXPERIMENTAL PROCEDURE

The holes that were examined were of ~6 mm in diameter and ~19 mm in length embedded in a tubular section made of high strength steel. The surface texture of the inside of the holes was probed using a modified COTS laser-based probe, the BEMIS SC™ Small Caliber Inspection System of Laser Techniques Company, Redmond, WA (ref. 3), as shown in figure 1. The tubular sections were positioned on X-Y stages for easy manipulation. The laser probe was aligned normal to the hole and centered as much as possible, and the start of the scans was at a 12 o'clock position of each hole. The linear and rotary resolutions were set at 50.8 and 25.4 µm, respectively. By experimentation, it was found that reproducible results were obtained when the laser power was set in auto mode and the detector gain was set at 5. The raw data files were imported to MATLAB for further signal processing. Some of the tubular sections were subjected to a safety and reliability test simulating storage conditions to withstand exposure to repeated cycles of extreme temperatures and humidity as per MIL-STD-331C test C1 (ref. 7). The tubular sections were exposed to a 28-day (two 14-day cycles) schedule of temperature and humidity variations to induce corrosion in the steel. The temperature extremes were +71° and −54°C, and a relative humidity of 95% was used at +71°C. As a rule of thumb, this testing in an unpackaged configuration is considered equivalent to 2 years of storage in an uncontrolled environment (ref. 8). The tubular sections were subjected to a total of three 28-day cycles for an equivalent exposure of 6 years in an uncontrolled environment and were scanned after 28, 56, and 84 days. Following the treatment, the corrosion build-up inside the holes was removed using brass bore brushes and ultrasonic cleaning. Due to the increased corrosion residue buildup after the 84-day treatment, stainless steel brushes in place of brass and a more rigorous cleaning cycle were employed compared to the 28 and 56-day treatments. This cleaning method was repeated as needed such that most of the corrosion residue was removed and the scan results did not vary appreciably after successive cleaning steps.
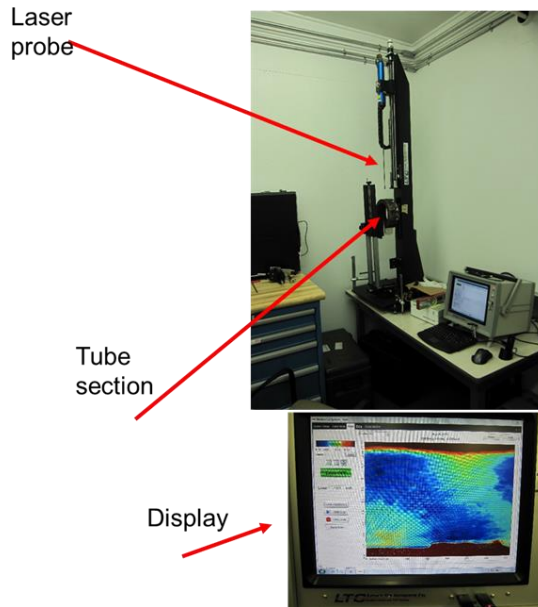
Figure 1
Experimental setup of probing the inside surfaces of holes in a steel tubular section using a modified
COTS laser-based probe

RESULTS AND DISCUSSION

Prior to extracting statistical information of surface features, the following operations were first applied to the raw scan data:

- Each scan consisted of a raster of measured radii $r(z, \theta)$ as a function of linear dimension (z) and angle (θ). Minimum and maximum values for linear dimension (z) were selected, and the scan is clipped to these bounds to limit the analysis to points inside the hole. While there is some inherent subjectivity in this task, every attempt was made to remain as consistent as possible. The plot in figure 2 illustrates the chosen limits for a particular scan.

Figure 2
Plot illustrating the chosen limits (the dotted lines) for a particular scan

- After clipping, each scan was median filtered by applying a two-dimensional median filter. That is, each pixel r[n, m] is replaced with the median value of the following set of points {r[n, m], r[n-1, m], r[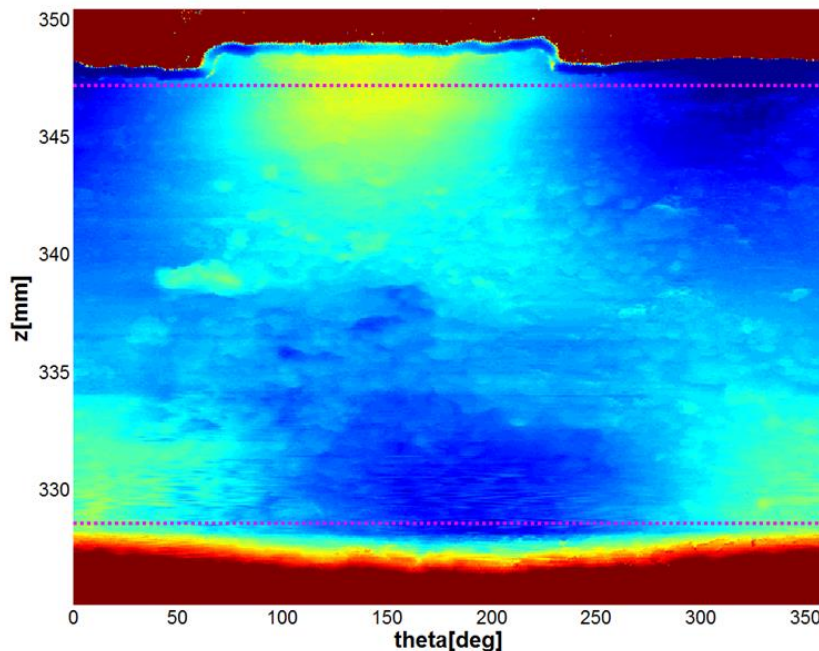n+1, m], r[n, m-1], r[n, m+1]}. This operation is quite effective in removing the speckle noise (i.e., isolated single point outliers) that is most likely associated with the measurement instrument.

- A correction was applied to the measured radii to correct for the probe deviation off the center axis of the hole. At each slice in z, an ellipse was fit to the measured radii. Each radius measurement was then replaced with the distance to the center of the ellipse, which was taken as the true axis of rotation. The parameters of this ellipse were estimated by minimizing the sum of the squared algebraic distances. If the parameters of the ellipse are denoted as $a = [a, b, c, d, e, f]$ and the sampled points by $\{p_1, p_2, \ldots p_N\}$ with $p_n = (x_n, y_n)$, then the parameters are estimated by finding the coefficients that minimize the following:

$$\sum_{n=1}^{N} F(a, p_n)^2 \qquad (1)$$

where $F(a, p_n) = ax_n^2 + bx_ny_n + cy_n^2 + dx_n + ey_n + f = 0$. This method appears to be effective in correcting the meandering of the probe as it goes through the hole. For example, shown in figure 3a, is a scan that illustrates the effects of a slight probe wander. Because the probe is slightly off the center axis of the hole, the measured radius is larger at certain angles and smaller at others. After applying the ellipse fitting technique, the resulting scan is much more cylindrical while still retaining much of the small-scale features as shown in figure 3b.
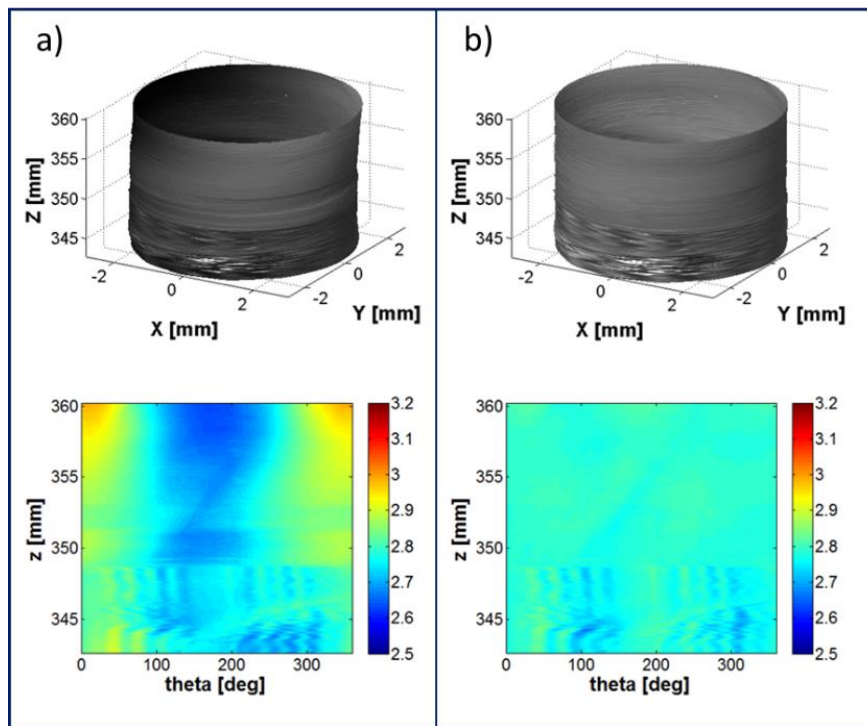
(a)
Scan showing effects of
probe wander as the probe
is slightly off the center
axis of the hole

(b)
Scan illustrating the
efficacy of the ellipse fitting
technique in removing
the probe wander

Figure 3
Effects of probe wander and ellipse fitting technique in removing probe wander

- After correcting for the probe wander, the angular values (θ) were replaced with an "unwrapped" linear dimension (x) using a nominal radius using the mapping $x = r_{ref}\theta$, [where r_{ref} was taken as 2.78 mm (nominal reference radius), and θ is the measurement angle in radians].

- The scan was resampled (using bicubic interpolation) for convenience to a common resolution in both x and z.

- It was also useful to filter out lower frequency components. A two-dimensional, circularly symmetric, low-pass filter was applied to the measurements to generate a background image consisting of the slowly varying components. The zero frequency component was retained in order to put the resulting signal on the same scale as the original (i.e., around 2.78 mm). This was accomplished by removing all spatial frequencies less than $0.25\ mm^{-1}$ in all directions via spatial filtering. Since potential pits are expected to be highly localized in space (high spatial frequency) and because of the possibility of longer wavelength variations (e.g., deviations in the geometry of the hole, remaining probe wander), this background provided a convenient baseline, removing any slowly varying spatial components to compare the measured radii for detection of pits.

- A binary image was formed from the measured radii that are at a given threshold above the background image.

- A single pixel above the background is most likely not a pit. To remove these potential false positives, a morphological "opening" operation is performed to the previously generated binary image. This consisted of "erosion" (retaining only points such that all points in a stencil are present) followed by "dilation" (retaining points with any point in a stencil being present). What this operation accomplishes is to remove groups of points below a given radius.

- The remaining points in the binary image are then associated to common pits. In order to associate pixels together, a criteria for connectedness is required. The criteria chosen was 8-connected (i.e., a pixel r[n, m] can be connected to a set of pixels if any of its eight surrounding neighbors are a member of the set).

Figure 4 illustrates successively processed plots of the original measurement after steps 6 (fig. 4a), 7 (fig. 4b), 8 (fig. 4c), and 9 (fig. 4d). Figure 4a shows the successively processed plots after background image determination by removing all spatial frequencies less than 0.25 mm^{-1} in all directions via fast Fourier transform filtering. Figure 4b shows the successively processed plots forming a binary image from the measured radii that are above a threshold of 0.125 mm. Figure 4c shows the successively processed plots after a morphological operation of the binary image shown in figure 4b. Figure 4d shows the association of points to common pits using the 8-connected criteria.
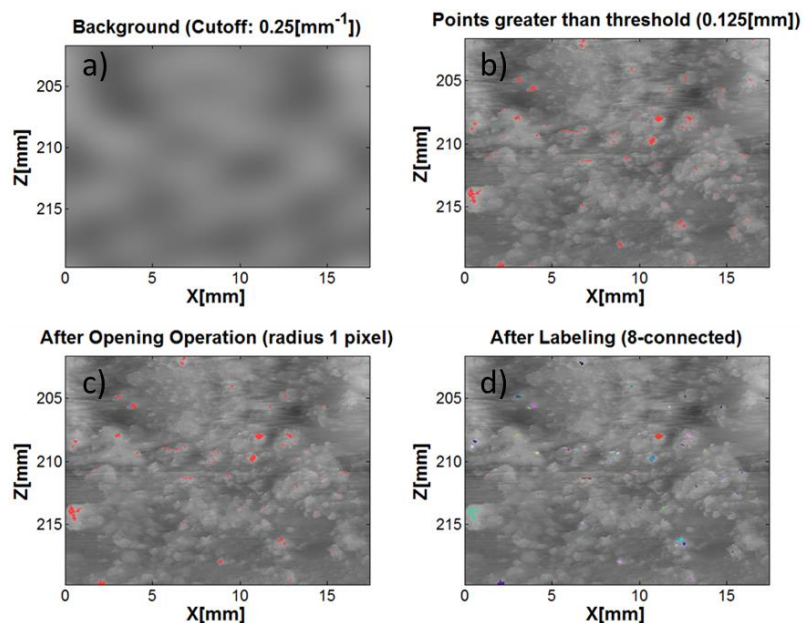
Figure 4
Successively processed plots of the original measurement

Scan Statistics

The effects of the corrosion treatments on the inside surfaces of the holes can be best captured using the statistical information of various surface texture parameters as defined in the International Organization for Standardization (ISO) 25178 for quantification of areal surface texture (refs. 9 and 10). The cumulative distribution of surface heights as a function of percentile can be illustrated via the Abbott-Firestone curves (refs. 9 and 10) after applying all of the previously mentioned operations of clipping, median filtering, correcting for probe wander, unwrapping, and removing low frequency components have been applied. Figure 5 shows the Abbott-Firestone

curves for a hole after corrosion treatment for 28, 56, and 84 days in comparison to the initial condition illustrating the increase in surface heights with the number of days of treatment. It can be seen that at lower percentiles (e.g., 5th through 10th), the surface height tends to increase with time illustrating the likelihood of the formation of pits. It was observed that the maximum surface height, however, is not necessarily always after the longest (i.e., 84 days) treatment suggesting perhaps that there is material buildup covering large peaks and that the post-corrosion cleaning process is not adequate in removing the corrosion residue completely. However, there is a clear widening of the distribution of material with respect to the number of days of treatment, exhibiting both large heights (potential pits) as well as low heights (buildup of material) at longer times.
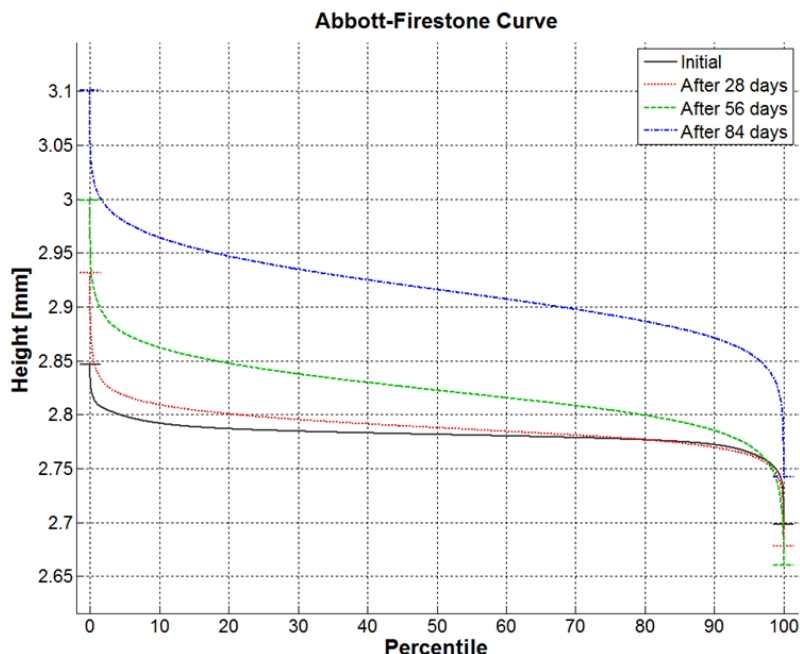

Figure 5
Abbott-Firestone curves of a hole that is subjected to corrosion treatment for 28, 56, and 84 days

Pit Definition

Identification of pits inside the holes, especially after the corrosion treatment, is an important engineering problem in assessing the engineering life of structures as most often surface flaws such as cracks are initiated at corrosion pits (ref. 6). There is, however, a great deal of difficulty in ascertaining what constitutes a "pit" in a given laser scan of the inside surface features of a hole, particularly when the pit is located deep inside the hole and not readily available for visible inspection. Clearly, a pit should be localized in space and should have a sufficient height. The requirement that pits be localized in space is one of the primary reasons for removing lower frequencies (i.e., spatial frequencies less than 0.25 mm^{-1}).

There are several parameters that affect the number of pits detected. The most critical of which are: (1) detection threshold value, (2) size of morphological "opening" stencil, and (3) criteria for connectedness. In order for a pixel to be classified as a potential pit, the pixel's value must exceed the background image by a value greater than or equal to the detection threshold. To get realistic values for the detection threshold, a tubular section that had been exposed to the environment for several years was cut open and the pit depths were obtained using an optical comparator. An inspection putty was used to form a mold of the cut opened hole surface, and after ~15 min, the surface features were impressed on the putty. The optical comparator scan of the putty

surface indicated that the deepest pit is of the order of 0. 675 mm and the smallest pit is of the order of 0.125 mm. The laser scan results from this section, obtained by using a threshold of 0.125 mm, spatial filter of 0.25 mm^{-1}, and a morphological opening stencil of 1 pixel radius, showed that the maximum and minimum pit depths were 0.683 and 0.131 mm, respectively. The maximum value is remarkably close to that obtained by the optical comparator demonstrating high accuracy of the laser scan method in pit depth determination. The pit distributions were computed for all the tubular sections tested in the study setting thresholds at ~0.075, 0.125, and ~0.25 mm. For the results presented in figure 6, unless otherwise stated, the following parameters were held constant:

- Bandwidth of low-pass filter: 0.25 mm^{-1}

- Morphological opening stencil used (radius 1 pixel): $\begin{bmatrix} 010 \\ 111 \\ 010 \end{bmatrix}$

- Connectedness: 8-connected
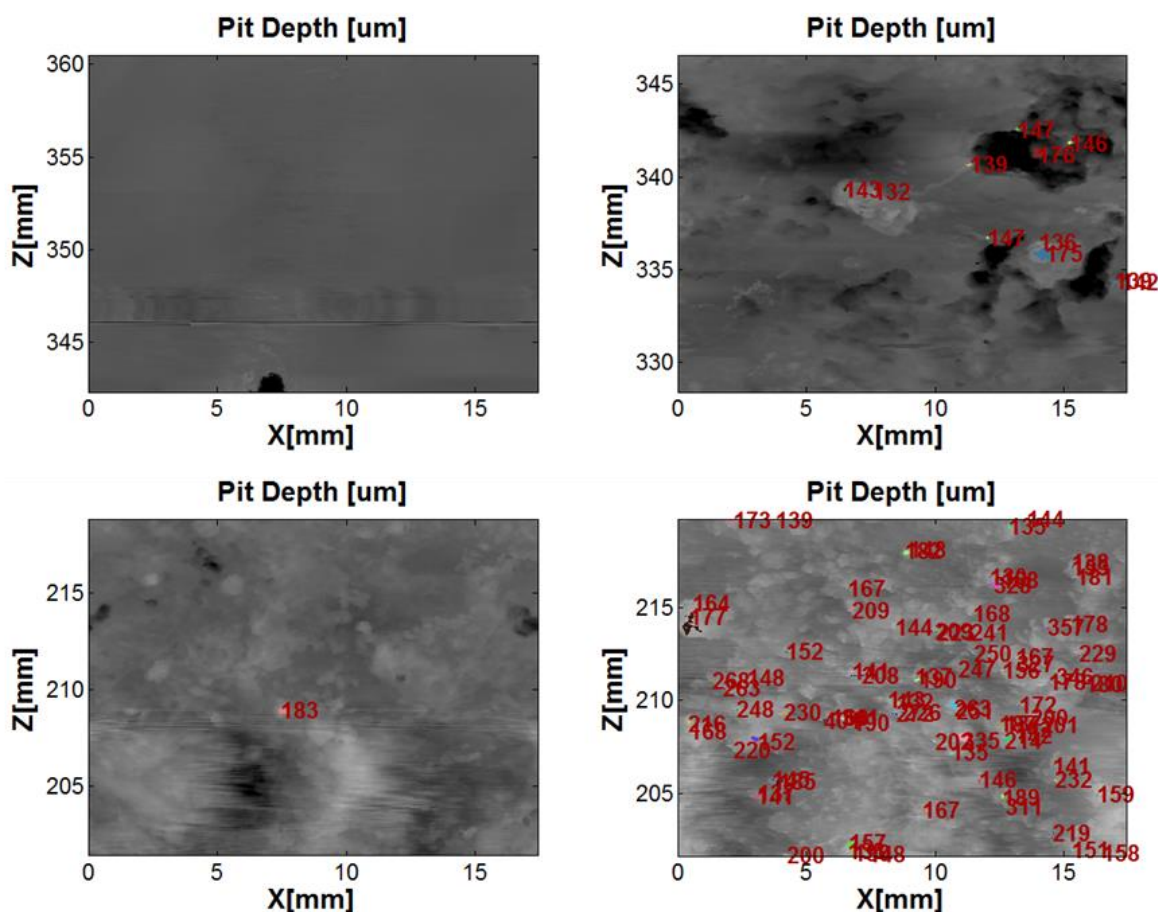
Figure 6
Binary images showing the progression of pit formation with the number of days of treatment for the same hole in a tubular section

The progression of the pit formation as a function of the number of days of treatment is illustrated in figure 6. The increased density of pits greater than 0.125 mm (threshold) after the 84-day treatment is clearly seen in the figure. The top left image is the initial, the top right is after 28 days, the bottom left is after 56 days, and the bottom right is after 84 days. The increased pit density after 84 days treatment is clearly noticed in the bottom right image. The numbers on the images

denote the pit depths. For these images, the threshold was set at 0.125 mm and the morphological opening stencil of 1-pixel radius was used.

The effects of the threshold and the morphological opening stencil radius on the pit distribution were examined. Figure 7 illustrates the effect of the threshold value on the ensuing pit distribution inside a hole of a tubular section after the 84-day treatment applied to the same scan data. Points that exceed the background protrude through the surface as illustrated in figure 7, and the effect of the three different thresholds (0.25, 0.125, and 0.075 mm) on the ensuing pit distribution is clearly seen. Figure 8 illustrates the effect of the varying threshold for a fixed morphological opening stencil radius (1 pixel) and varying morphological opening stencil radius for a fixed threshold (0.125 mm) on the number of pits for the scan data from one of the tubular sections after the 84-day treatment. The top plot in figure 8 illustrates the effect of threshold on the number of pits for a morphological opening stencil of 1-pixel radius. The bottom plot shows the effect of varying the morphological opening radius on the number of pits for a threshold value of 0.125 mm. Both the plots were derived from the same scan data from one of the tubular sections in the original condition and after the 28, 56, and 84-day treatments. The progressive increase in the number of pits with increasing number of treatment days clearly evince the increased corrosion.
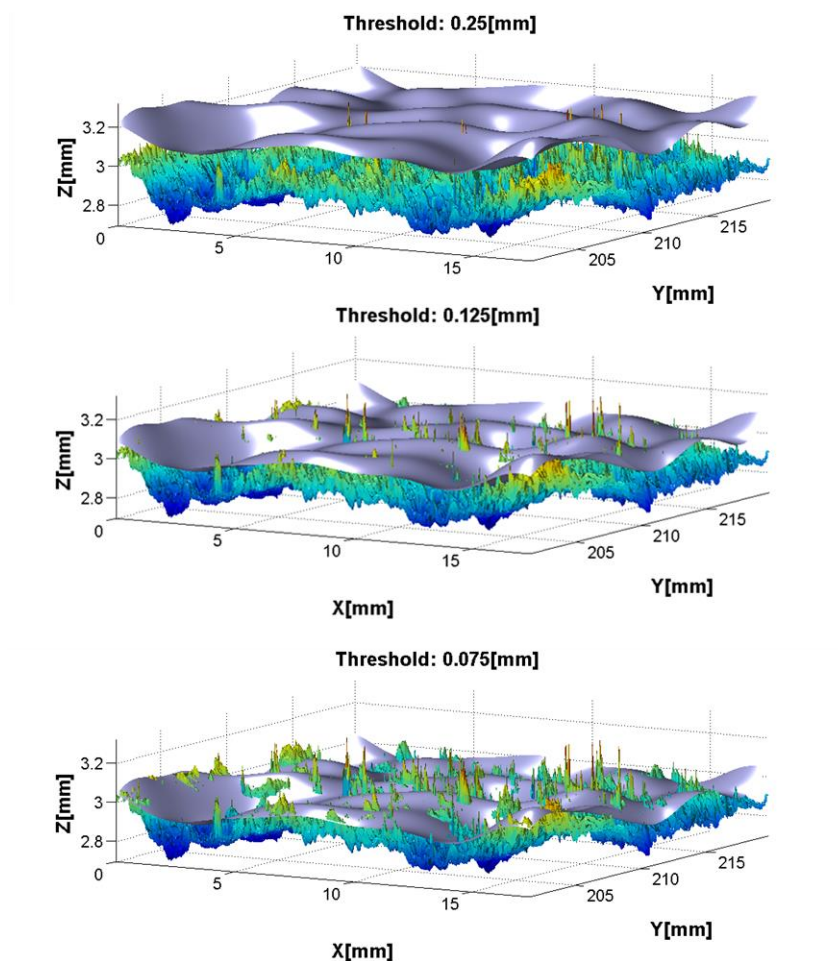

Figure 7
Pit distribution inside a hole of a tubular section after the 84-day treatment for three different thresholds
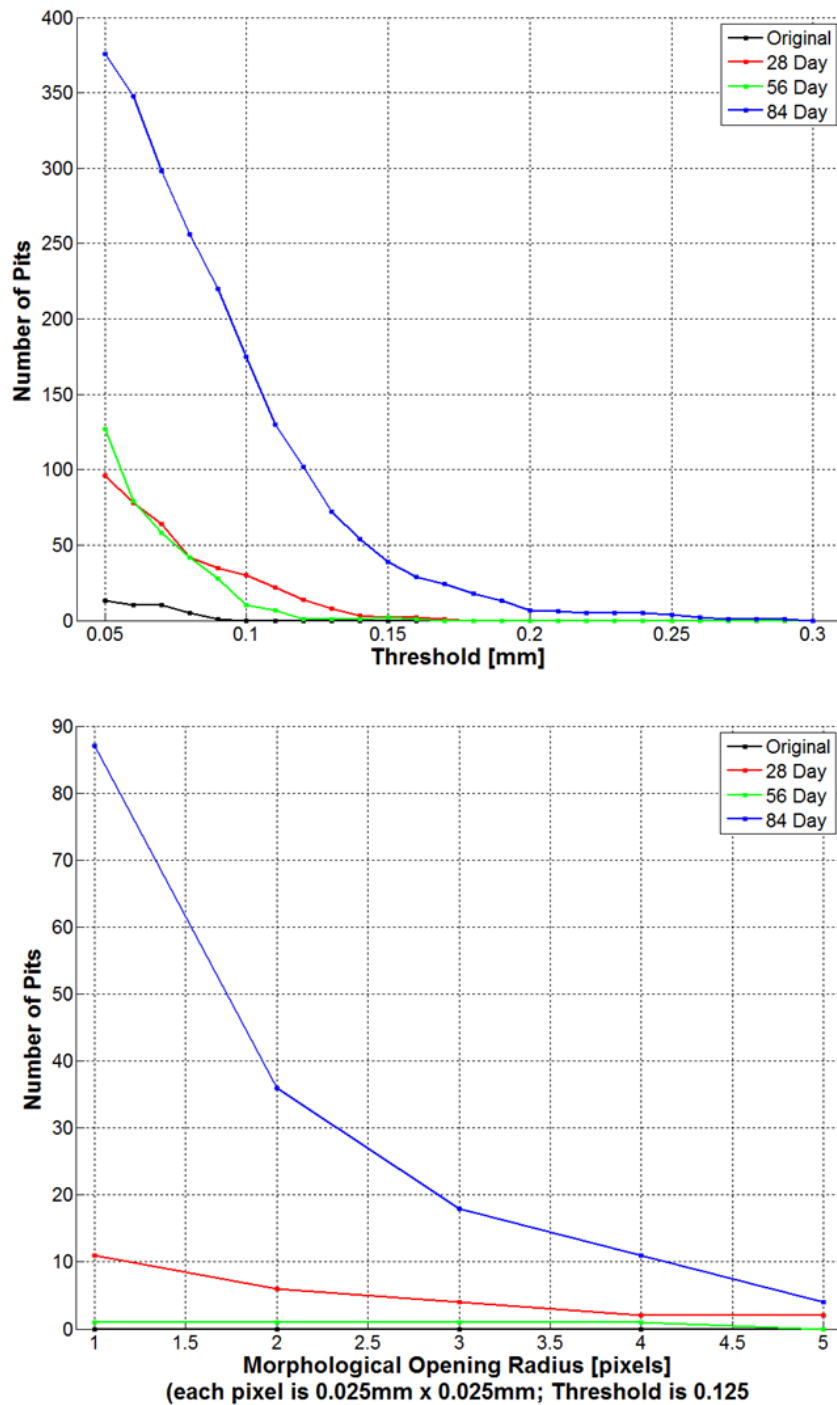
Figure 8
Effect of the varying threshold for a fixed morphological opening stencil radius (1 pixel) and varying morphological opening stencil radius for a fixed threshold (0.125 mm)

Finally, figure 9 illustrates the pit density as a function of pit depth for the different number of treatment days derived from the data obtained from all 15 of the tubular sections examined in the study. The number of pits for a morphological opening stencil of 1-pixel radius is calculated in 25-µm bins, and this is divided by the total area to compute the pit density in each bin. The number of pits in

the 25-µm bins is shown at the bottom of the figure. A few observations can be made: (1) pit density decreases monotonically with increasing pit depth, (2) the maximum pit depth beyond which the pit density is negligible increases with the number of treatment days, and (3) for a given pit depth below the maximum, the pit density increases with the number of treatment days. For example, for a pit depth of 0.1 mm, the pit density increases by ~2.5 and ~4.5 times, respectively, after 56 and 84 days compared to that after 28 days of treatment. Given that the environment test of temperature and humidity exposure used in the study is equivalent to ~2 years of uncontrolled environment, it may be surmised that for every two years of exposure, the growth rate of pits is approximately doubled.
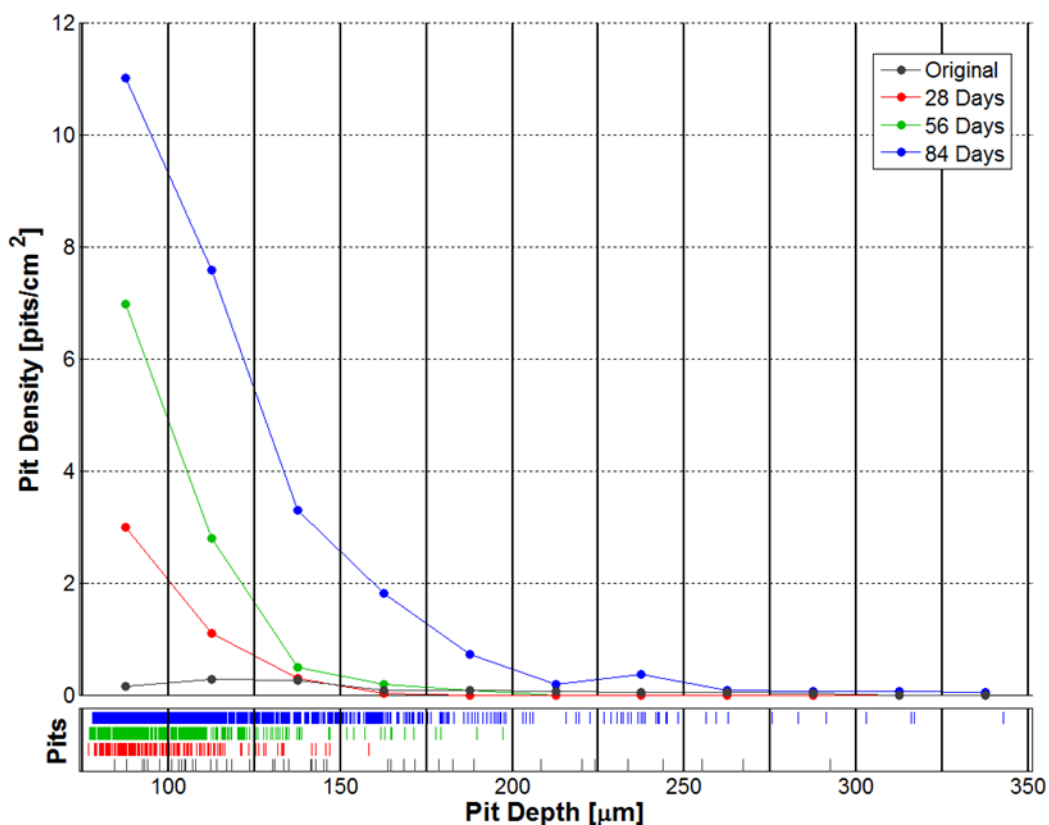

Figure 9
Plot of pit density as a function of pit depth for different number of treatment days

CONCLUSIONS

A modified commercial off-the-shelf laser based probe was applied, the BEMIS SC™ Small Caliber Inspection System of Laser Techniques Company, Redmond, WA, to nondestructively examine the inside surface texture of holes ~6 mm in diameter and ~19 mm in length embedded in a tubular section made of high strength steel. The data was analyzed using a signal processing algorithm developed in MATLAB that included: (1) correction for the laser probe wander of the center axis of the hole, (2) a low-pass filter to remove any slowly varying spatial components and provide a convenient reference surface, (3) determination of surface pits that are above a give threshold value, (4) a morphological operation to remove potential false positives, and (5) a criteria of connectedness to associate pixels to common pits. The tubular sections were subjected to a 28-day (two 14-day cycles) schedule of temperature and humidity variations to induce corrosion in the steel. The temperature extremes were +71° and −54°C, and a relative humidity of 95% was used at +71°C. The cumulative distribution of surface heights as a function of percentile, illustrated via the Abbott-

Firestone curves, revealed that the surface height tends to increase with the number of days of treatment suggesting the formation of pits. Further analysis of the pit distributions showed that the pit density decreases monotonically with increasing pit depth, the maximum pit depth beyond which the pit density is negligible increases with the number of treatment days, and for a given pit depth below the maximum, the pit density increases with the number of treatment days. For example, for a pit depth of 0.1 mm, the pit density increases by ~2.5 and ~4.5 times, respectively, after 56 and 84 days compared to after 28 days of treatment. No surface defects such as cracks were observed in any of the sections even after the 84-day treatment.

REFERENCES

1. Duran, O., Althoefer, A., and Seneviratne, L.D., "Pipe inspection using a laser-based transducer and automated analysis techniques," IEEE/ASME Transactions on Mechatronics, vol. 8, pp. 401-409, 2003.

2. Tsubouchi, T., Takaki, S., Kawaguchi, Y., and Yuta, S., "A straight pipe observation from the inside by laser spot array and a TV camera," Proceedings of the IEEE/RSJ International Conference on Intelligent Robots and Systems, pp. 82-87, 2000.

3. http://www.laser-ndt.com/products.html

4. Kim, H.S., Lee, B.R., and Kim, R.J., "Development of computer-vision-based pipe inspection system," IEEE Proc. of the 1st International Forum on Strategic Technology, pp. 403-406, 2006.

5. Zhang, G., He, J., and Li, X., "3D vision inspection for internal surface based on circle structures light," Sensors and Actuators A, vol. 122, pp.68-75, 2005.

6. Fang, B.Y., Eadie, R.L., Chen, X.X., and Elboujdaini, M., "Pit to crack transition in X-52 pipeline steel in near neutral pH environment: Part 1 – formation of blunt cracks from pits under cyclic loading," Corrosion Eng. Sci. Tech., vol. 45, pp.302-312, 2010.

7. Department of Defense Test Method Standard, "Fuze and Fuze Components, Environmental and Performance Tests For," MIL-STD-331C w/Change 1, dated 22 June 2009.

8. Gagliardi, F.A., Private communication, U.S. Army ARDEC, Picatinny Arsenal, NJ, 07806.

9. ISO 25178-1, "Geometrical product specifications - Surface texture: Areal - Part 1: Indication of surface texture," 2015.

10. ISO 25178-2, "Geometrical product specifications - Surface texture: Areal - Part 2: Terms, definitions and surface texture parameters," 2012.

DISTRIBUTION LIST

U.S. Army ARDEC
ATTN: RDAR-EIK
         RDAR-MEF,   V. Swaminathan
         RDAR-MEF-P,   D. Grasing
         RDAR-WSW-F,   A. Foltz
         RDAR-MEM-M,   R. Hooke
Picatinny Arsenal, NJ 07806-5000

Defense Technical Information Center (DTIC)
ATTN: Accessions Division
8725 John J. Kingman Road, Ste 0944
Fort Belvoir, VA 22060-6218

GIDEP Operations Center
P.O. Box 8000
Corona, CA 91718-8000
gidep@gidep.org

U.S. Army ARDEC, Benét Laboratory
ATTN: RDAR-WSB-L,   A. Littlefield
Watervliet, NY 12189-4000

REVIEW AND APPROVAL OF ARDEC REPORTS

THIS IS A:

[✓] TECHNICAL REPORT   [ ] SPECIAL REPORT

[ ] MEMORANDUM REPORT   [ ] ARMAMENT GRADUATE SCHOOL REPORT

ARDEC 6.2

FUNDING SOURCE
(e.g., TEX3, 6.1 (ILIR, FTAS); 6.2; 6.3; PM funded BMD; PM funded Production/ESIP; Other (please identify))

Nondestructive assessment of inside surfaces of cast beats in a steel structure using a laser scan technique

Title	Project

Venkataraman Swaminathan   ARMET-TR-17031

Author/Project Engineer	Report number/Date received (to be completed by LCSD)

4-7455   B407   RDAR-MEF

Extension	Building	Author's Office Symbol

PART 1   Must be signed before the report can be edited.

a.   The draft copy of this report has been reviewed for technical accuracy and is approved for editing

b.   Use Distribution Statement A ✓ , B____ , C____ , D____ , E____ , or F____ for the reason checked on the continuation of this form. Reason: _____

    1   If Statement A is selected, the report will be released to the National Technical Information Service (NTIS) for sale to the general public. Only unclassified reports whose distribution is not limited or controlled in any way are released to NTIS.

    2   If Statement B, C, D, E, or F is selected, the report will be released to the Defense Technical Information Center (DTIC) which will limit distribution according to the conditions indicated in the statement.

c.   The distribution list for this report has been reviewed for accuracy and content, 1998.

Douglas C. Troast

Division Chief	(Date)

PART 2.   To be signed either when draft report is submitted or after review of reproduction copy.

This report is approved for publication

Douglas C. Troast   28 Mar 17

Division Chief	(Date)

Andrew Pskowski   4/4/17

RDAR-CIS	(Date)

LCSD 49 (1 Sept 16)
Supersedes SMCAR Form 49, 20 Dec 06